Journal of Sound and Vibration (2000) **231**(4), 1111–1134
doi:10.1006/jsvi.1999.2725, available online at http://www.idealibrary.com on IDEAL®

ANDERSON LOCALIZATION IN COUPLED REVERBERATION ROOMS

R. L. Weaver and O. I. Lobkis

Theoretical & Applied Mechanics, 104 *So Wright Street*, *University of Illinois*, *Urbana*, *IL* 61801, *U.S.A.*

(*Received* 22 *July* 1999, *and in final form* 20 *September* 1999)

It is shown that energy flow between weakly coupled reverberant systems, for example reverberation rooms coupled by a small window, can be Anderson localized. The effect is significant when the energy flow rate (in units of inverse time) is comparable to or less than modal spacings. It is found that the energy partition in the localized regime slightly overshoots its (low) asymptotic value. The effect is demonstrated in numerical simulations and in a laboratory ultrasonic system.

1. INTRODUCTION

The transient flow of diffuse vibrational energy between coupled substructures is often modelled by means of an analysis similar to that of statistical energy analysis (SEA) [1–3]. In this approach the energy in each substructure is thought to dissipate at a rate particular to that substructure, and to diffuse from one to the other at a rate proportional to the difference in energy per mode and proportional to a symmetric coupling constant.

In a pair of widely quoted papers, however, Hodges [4, 5] pointed out that if the vibrational eigenmodes of the whole structure are Anderson localized, then diffusion cannot take place. Indeed, energy originally placed in one eigenmode must stay in that mode. Only the modes localized near the source will be excited by the source, the receiver can detect only excitation in the modes localized near it. If the receiver and source are well separated, the response is negligible—*regardless of dissipation or the lack thereof, and regardless of the amount of time one waits for the diffuse signal to arrive*. The appealing analogy, between the transport of diffuse vibrations and the conductive transport of heat, is not reliable.

There have been numerous demonstrations of localization of vibrations in quasi-one-dimensional structures [6–8] for which localization is relatively common, and other demonstrations of the transition between diffusion and localization in multi-coupled one- and two-dimensional disordered structures [9–13] for which localization is weaker. In all this work it appears that the simplest model in which that transition can occur has been neglected. It is our hypothesis that this system is interesting in its own right, and also that study of this simple system can inform our understanding of more complex systems.

0022-460X/00/141111 + 24 $35.00/0

In this paper, we study a few versions of the classic problem of coupled reverberation rooms. The predictions of an SEA-like model in which energy diffuses between the rooms is contrasted with a theoretical calculation in which energy is localized in one room. Numerical simulations of vibrations in a two-dimensional finite difference model of coupled reverberation rooms, and laboratory experiments on weakly damped coupled elastic bodies, confirm the theoretical arguments.

2. STATISTICAL ENERGY ANALYSIS FOR TRANSIENT ENERGY FLOW

An SEA-like model of transient energy flow [2, 3] between two undamped rooms of equal volume and equal modal density suggests that the following equations should describe the evolution of energy densities:

$$\mathrm{d}E_1/\mathrm{d}t = \Pi(t) - \sigma(E_1 - E_2), \qquad \mathrm{d}E_2/\mathrm{d}t = -\sigma(E_2 - E_1), \tag{1}$$

where E_i is the spectral energy density in substructure i at the frequency of interest. Figures 1 describe the physical systems which are modelled here. Equation (1) describes the deposition of energy in substructure number 1 by a source with power Π, and its leaking into substructure number 2 at a rate proportional to the difference in energy per mode. An initial impulsive unit energy deposit in region 1 leads to an eventual state with equal amounts of energy in each substructure,

$$E_1(t) = (1/2)[1 + \exp\{-2\sigma t\}], \qquad E_2(t) = (1/2)[1 - \exp\{-2\sigma t\}]. \tag{2}$$

A ray-acoustic model suggests that the leaking rate σ may be estimated, in the case that the substructures are rooms coupled through a transparent window of area A, to be

$$\sigma = Ac/4V_{\mathrm{ol}}, \tag{3}$$

where V_{ol} is the volume of each room and c is the wave speed.

Such a model depends on the ray-acoustic picture, which in turn is acceptable only for wavelengths sufficiently short compared to the window size. Nevertheless, it is the SEA conceit that equations like equation (1) should still apply, not withstanding the admitted greater difficulty in estimating leak rates by considering diffraction at the window.

The SEA conceit is incorrect. Energy flow in undamped systems must cease after a time of the order of the modal density, because time evolution in the diffuse field must be a product of beating between nearby modes. If D is the modal density (modes per unit frequency $\mathrm{d}N/\mathrm{d}\omega$ where N is the smoothed modal count (staircase) function) then the notion that time scales of the flow must be no greater than the modal density, coupled with an assumption that the time scale of the flow is the leaking rate σ (i.e., that the leaking continues until equipartition) suggests that leaking rates σ must be greater than or equal to a quantity of order $1/2\pi D$. As $D \sim V_{\mathrm{ol}}\,\omega^2/2\pi^2c^3$ one concludes, by comparison with equation (3), that there is

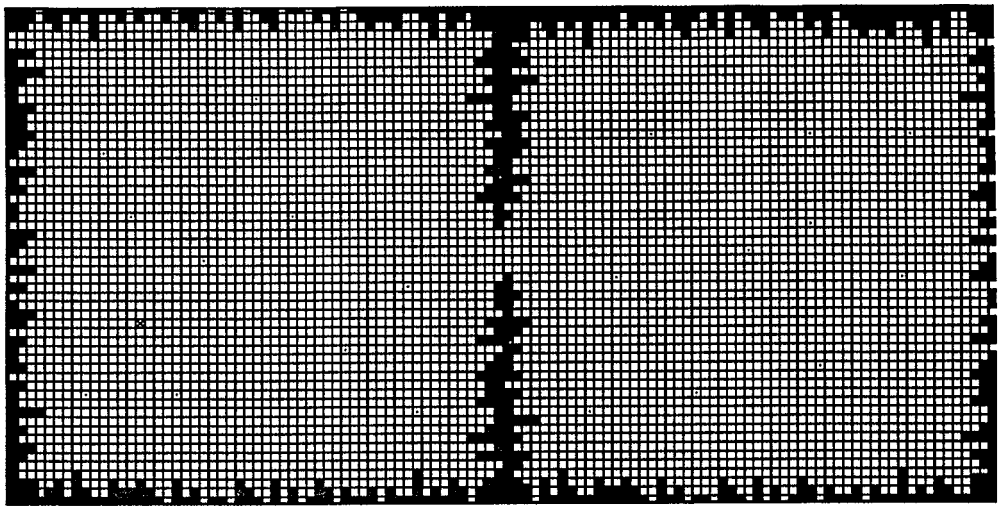

(a)

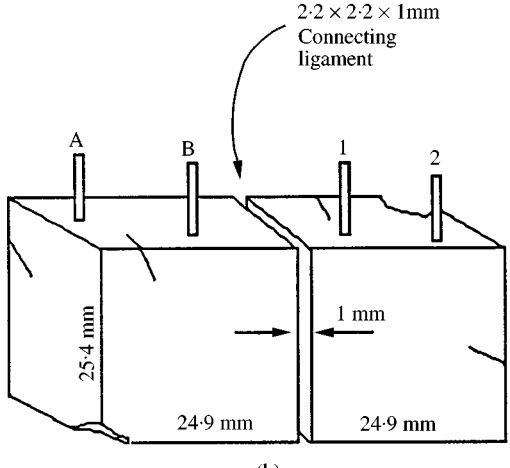

(b)

Figure 1. The system considered consists of two lightly coupled reverberant bodies. (a) The numerics simulated the dynamics of two meshes of unit point masses all attached to the intersections of unit-tensioned strings. The meshes were given rough boundaries, as sketched. In the first numerical study they were coupled by means of a short window. The source site is indicated by a small star; the many receiver sites are indicated by dots. In another simulation (not pictured) the meshes were coupled by 12 light springs, connecting sites of one mesh with the corresponding sites of the other. (b) Aluminum block used for laboratory confirmation of the effect. It had four distinct and nominally identical dry-coupled sources/receivers attached, two on each side. A small ligament of dimensions 2·2 × 2·2 × 1·0 mm near the centre of the gap acts as a window and connects the two sides acoustically.

a critical frequency below which SEA must fail. ω_{crit} is the solution of $\sigma = Ac/4V_{ol} = 1/2\pi D$, i.e., $\lambda_{crit} = (A\pi)^{1/2}$. Except for a numerical factor of order unity, this cutoff is the same as that of diffraction corrections in the ray-acoustic picture.

An alternative argument that leads to the same result is provided by applying perturbation theory to the eigenvalue problem of coupled rooms. The coupling mixes the modes of the separate rooms. It is well known that, at leading order, perturbation theory indicates that modes mix well only if the coupling is in some sense comparable to or stronger than the unperturbed spacing between the original modes. Perturbation theory itself is manifestly valid only if the ratio of coupling to spacing is small. Thus, for large spacing (i.e., low modal density) compared to coupling strength (which presumably may be quantified by the nominal leaking rate σ), i.e., for small $D\sigma$, we expect the typical mode of the composite to be localized in one room or the other. One again concludes that equipartition cannot take place at low values of $D\sigma$.

That SEA fails at low modal density is generally conceded. We see that the failure here is not for low modal density *per se*, nor for modal density low compared to absorption time (equivalent to low modal overlap.) The critical parameter is modal density times coupling rate.

This lack of equipartition in weakly coupled reverberation rooms is a kind of Anderson localization, albeit for a zero-dimensional multi-coupled system. The critical quantity $D\sigma$ is similar to Thouless dimensionless conductance [14] in that the physical conductance is the leaking rate σ; it is non-dimensionalized by the modal density. It is also related to the inverse of Anderson's W/V parameter [15], the ratio of disorder W to coupling strength V. Coupling strength is characterized by the leaking rate, and disorder by the typical spacing between pseudo-modes of the separate rooms, i.e., the inverse of the modal density.

In this paper, we shall study the energy flow between two such reverberation rooms, and in particular scrutinize the behavior as the critical frequency is exceeded, or not.

3. A MODAL PICTURE OF TRANSIENT ENERGY FLOW

We consider a structure governed by the following differential equation:

$$\frac{\partial^2 \mathbf{U}(t)}{\partial t^2} = \boldsymbol{C}\,\mathbf{U}(t) + \delta(t)\mathbf{S}, \tag{4}$$

where $\boldsymbol{C}$ is a self-adjoint operator and $\mathbf{U}$ and $\mathbf{S}$ are vectors in the Hilbert space. $\mathbf{S}$ is the source distribution and $\mathbf{U}$ is the response. With the understanding that we are interested in the response within a narrow band of frequencies centered on $\omega \sim \Omega$, it suffices to write

$$\mathbf{U}(t) = \mathbf{u}(t)\exp(-\mathrm{i}\Omega t), \tag{5}$$

where $\mathbf{u}$ is slowly varying in time. We can then approximate the governing ordinary differential equation (ODE) as a Schrodinger equation

$$-\mathrm{i}\partial_t \mathbf{u} = \frac{1}{2\Omega}\boldsymbol{C}\mathbf{u} + \frac{1}{2\Omega}\mathbf{S}\delta(t) = [\boldsymbol{H}_1 + \boldsymbol{H}_2 + \boldsymbol{v}]\mathbf{u} + \mathbf{s}\delta(t). \tag{6}$$

This transformation is not necessary for the purposes at hand, but it does simplify the subsequent analysis. We have furthermore pictured $\boldsymbol{C}$ as nearly block-diagonal, and decomposed it as the sum of distinct self-adjoint operators $\boldsymbol{H}_1$ and $\boldsymbol{H}_2$ and a (presumed small) coupling term $\boldsymbol{v}$. $\boldsymbol{H}_i$ is taken to be the operator that governs the dynamics of room number i. H_1 has eigenvectors ψ^n with eigenvalues ω_n; $\boldsymbol{H}_2$ has eigenvectors ϕ^v with eigenvalues α_v.

$$\begin{gathered}\boldsymbol{H}_1\boldsymbol{\psi}^n = \omega_n\boldsymbol{\psi}^n, \qquad \boldsymbol{H}_2\boldsymbol{\phi}^v = \alpha_v\boldsymbol{\phi}^v, \\ \boldsymbol{\psi}^n\cdot\boldsymbol{\psi}^m = \delta_{nm}, \qquad \boldsymbol{\phi}^v\cdot\boldsymbol{\phi}^\mu = \delta_{v\mu}, \qquad \boldsymbol{\psi}^n\cdot\boldsymbol{\phi}^v = 0,\end{gathered} \tag{7}$$

where $\cdot$ signifies an inner product. ψ^n and ϕ^v are not modes of the entire system, but can be termed pseudo-modes, they nearly satisfy the governing equations, and do span the space. For simplicity, we take $\boldsymbol{v}$ to be purely off-block-diagonal. This entails no loss of generality as we may define $\boldsymbol{H}$ to include the block diagonal portion of $\boldsymbol{v}$. Thus

$$\boldsymbol{\phi}^v\cdot\boldsymbol{v}\boldsymbol{\phi}^\mu = \boldsymbol{\psi}^n\cdot\boldsymbol{v}\boldsymbol{\psi}^m = 0. \tag{8}$$

The off-diagonal parts of $\boldsymbol{v}$ do not, however, vanish:

$$\boldsymbol{\phi}^v\cdot\boldsymbol{v}\boldsymbol{\psi}^n = \boldsymbol{\psi}^n\cdot\boldsymbol{v}\boldsymbol{\phi}^v \equiv V_{nv}. \tag{9}$$

We furthermore take the source to act only in room number 1; thus

$$\mathbf{s}\cdot\boldsymbol{\phi}^v = 0, \qquad \mathbf{s}\cdot\boldsymbol{\psi}^n \equiv s_n. \tag{10}$$

In the absence of coupling, $\boldsymbol{v} = 0$, our solution of equation (6) is

$$\mathbf{u} = \sum_n \exp\{\mathrm{i}\omega_n t\}\,\boldsymbol{\psi}^n(\boldsymbol{\psi}^n\cdot\mathbf{s}). \tag{11}$$

One finds that the response remains in room number 1. We can calculate, in each room, a quantity which we will call energy, $E = \mathbf{u}\cdot\mathbf{u} = E_1 + E_2$:

$$\begin{aligned}E_1 &= \sum_m |\mathbf{u}\cdot\boldsymbol{\psi}^m|^2 = \sum_m |\mathbf{s}\cdot\boldsymbol{\psi}^m|^2 = \mathbf{s}\cdot\mathbf{s}, \\ E_2 &= \sum_\mu |\mathbf{u}\cdot\boldsymbol{\phi}^\mu|^2 = 0,\end{aligned} \tag{12}$$

and find that they are constants.

If $\boldsymbol{v} \neq 0$ we write the solution in the form

$$\mathbf{u}(t) = \sum_n a_n(t)\boldsymbol{\psi}^n + \sum_v b_v(t)\boldsymbol{\phi}^v \tag{13}$$

and derive coupled ODEs for the coefficients a and b:

$$\begin{aligned} -\mathrm{i}\partial_t a_n &= \omega_n a_n + \sum_\mu V_{n\mu} b_\mu(t) + (\boldsymbol{\psi}^n \cdot \mathbf{s})\delta(t), \\ -\mathrm{i}\partial_t b_\mu &= \alpha_\mu b_\mu + \sum_n V_{n\mu} a_n(t). \end{aligned} \tag{14}$$

3.1. SOLUTION AT LEADING ORDER IN V

If $\boldsymbol{v}$ is in some sense small, it is reasonable to attempt a series solution in powers of V. To leading order one finds that $a(t)$ is independent of $\boldsymbol{v}$:

$$a_n(t) = \mathrm{i}(\boldsymbol{\psi}^n \cdot \mathbf{s})\exp\{\mathrm{i}\omega_n t\}\,\Theta(t), \tag{15}$$

where Θ is the unit step function. One also finds, at leading order, that b is governed by the simple ODE:

$$\partial_t b_\mu(t) = \mathrm{i}\alpha_\mu b_\mu - \Theta(t)\sum_n \exp(\mathrm{i}\omega_n t)\, V_{n\mu}(\boldsymbol{\psi}^n \cdot \mathbf{s}), \tag{16}$$

which has the solution

$$b_\mu(t) = \mathrm{i}\,\Theta(t)\sum_n \frac{\exp(\mathrm{i}\omega_n t) - \exp(\mathrm{i}\alpha_\mu t)}{(\omega_n - \alpha_\mu)}\, V_{n\mu}(\boldsymbol{\psi}^n \cdot \mathbf{s}). \tag{17}$$

We see that, to this order, E_1 is still given by equation (12), and E_2 may readily be calculated:

$$\begin{aligned} E_2 &= \sum_\mu |\mathbf{u}\cdot\boldsymbol{\phi}^\mu|^2 = \sum_\mu |b_\mu|^2 \\ &= \sum_\mu \sum_n \sum_{n'} \frac{(\exp\{\mathrm{i}\omega_n t\} - \exp\{\mathrm{i}\alpha_\mu t\})}{(\omega_n - \alpha_\mu)} \frac{(\exp\{-\mathrm{i}\omega_n t\} - \exp\{-\mathrm{i}\alpha_\mu t\})}{(\omega_{n'} - \alpha_\mu)}\, V_{n\mu} V_{n'\mu} s_n s_{n'}. \end{aligned} \tag{18}$$

The terms $n \neq n'$ have vanishing expectation $\langle V_{n\mu} V_{n'\mu}\rangle = \langle V^2\rangle \delta_{nn'}$. So

$$\langle E_2\rangle = \sum_\mu \sum_n \frac{4\sin^2[(\omega_n - \alpha_\mu)t/2]}{(\omega_n - \alpha_\mu)^2} \langle V^2\rangle s_n^2. \tag{19}$$

The sum over μ may be replaced with a factor of the modal density in room 2 and an integral over α:

$$\begin{aligned} \langle E_2\rangle &= \sum_n \langle V^2\rangle s_n^2 \int_{-\infty}^{\infty} D\,\mathrm{d}\alpha\, \frac{4\sin^2[(\omega_n - \alpha)t/2]}{(\omega_n - \alpha)^2} \\ &= 2\pi t D\langle V^2\rangle \sum_n s_n^2 = 2\pi t D\langle V^2\rangle E_1. \end{aligned} \tag{20}$$

Thus the initial leaking rate, $\sigma = 2\pi D\langle V^2\rangle$, is described in terms of the modal density D and the mean-square value of the off-block-diagonal elements of V. This result is valid for all systems of form (6), not just the ones for which we expect a ray-acoustic model or an SEA Ansatz to apply. The analysis is, however, a perturbative one in the strength of V. Even at small v it is apparent that the perturbation series solution of equations (14) will have secular terms and that equations (15)–(19) do not apply beyond early times. Application to later times requires that the series be extended to higher order. Nevertheless, the result indicates that the SEA conceit must be correct at early times *even at very low modal density*. Energy leaks at a simple initial rate proportional to modal density and to the coupling strength. Leaking rates can be arbitrarily slow. At low $D\sigma$ the energy densities will not (according to the arguments in the preceding section) asymptote to equipartition, but there is, apparently, no indication of that during the early stages of the flow.

3.2. SOLUTION AT LOW D

Energy does not diffuse classically at low D, but it does flow. It remains an open question as to how the weak flow proceeds. To answer this we need a solution of equations (14) valid for all times. That is possible in a limit of very low modal density, i.e., in the localized regime.

In the localized regime the little energy that does flow is carried by mode pairs (ψ, ϕ) which happen to differ only slightly in frequency. Only these pairs mix well enough not to localize. An approximate solution to equations (14) may therefore be obtained by truncating the sums to a single term each, the mode of the adjacent room with the closest frequency α_μ to ω_n. Dropping the subscripts,

$$-\mathrm{i}\partial_t a = \omega a + bV + s\delta(t),$$

$$-\mathrm{i}\partial_t b = \alpha a + aV,$$

or

$$-\mathrm{i}\partial_t \begin{Bmatrix} a' \\ b' \end{Bmatrix} = \begin{bmatrix} 0 & V \\ V & \alpha - \omega \end{bmatrix} \begin{Bmatrix} a' \\ b' \end{Bmatrix} + \begin{Bmatrix} s \\ 0 \end{Bmatrix} \delta(t), \tag{21}$$

where a' and b' are equal to $ae^{-\mathrm{i}\omega t}$ and $be^{-\mathrm{i}\omega t}$ respectively. Standard methods for solutions of 2×2 symmetric systems give us a solution

$$\begin{Bmatrix} a' \\ b' \end{Bmatrix} = \frac{\mathrm{i}s}{V(\lambda_- - \lambda_+)} \left[\begin{Bmatrix} V \\ \lambda_+ \end{Bmatrix} \lambda_- \exp\{\mathrm{i}\lambda_+ t\} - \begin{Bmatrix} V \\ \lambda_- \end{Bmatrix} \lambda_+ \exp\{\mathrm{i}\lambda_- t\} \right], \tag{22}$$

where λ_+ and λ_- are the eigenvalues of the 2×2 matrix $[0\ V;\ V\ \alpha - \omega]$

$$\lambda_\pm = \frac{(\alpha - \omega) \pm \sqrt{(\alpha - \omega)^2 + 4V^2}}{2}, \tag{23}$$

b^2 is the energy in room 2 associated with the mode of frequency α,

$$|b(t)|^2 = |b'(t)|^2 = \frac{4s^2(\lambda_+\lambda_-)^2}{V^2(\lambda_- - \lambda_+)^2}\sin^2[(\lambda_+ - \lambda_-)t/2]$$

$$= s^2\frac{4V^2}{(\alpha-\omega)^2 + 4V^2}\sin^2[\sqrt{(\alpha-\omega)^2 + 4V^2}\,t/2], \qquad (24)$$

$|b|^2$ oscillates at the beat frequency $(\lambda_+ - \lambda_-)$.

The difference frequency $\alpha - \omega$ between the nearby modes of the two rooms is a random number, with spectral density D. We take an expectation of equation (24) by inserting a factor of D and integrating over all α. On also performing a sum over all modes in room 1 we obtain

$$\langle E_2\rangle = ED\int_{-\infty}^{\infty} d\alpha \frac{4V^2}{(\alpha-\omega)^2 + 4V^2}\sin^2[\sqrt{(\alpha-\omega)^2 + 4V^2}\,t/2]. \qquad (25)$$

On suitable variable change this becomes

$$\langle E_2\rangle = 2ED|V|\int_{-\infty}^{\infty} d\beta \frac{\sin^2(\sqrt{1+\beta^2}\,tV)}{1+\beta^2}. \qquad (26)$$

As $t \to \infty$ this is manifestly

$$\lim_{t\to\infty}\langle E_2\rangle/E = D\pi|V|. \qquad (27)$$

This is one of the central results of the present calculation. It is predicted, in the limit of low values for $D\langle V^2\rangle^{1/2}$, that the asymptotic level of energy in room 2 is less than that in room 1 by a factor of order DV. This is a prediction that is subject to corroboration in numerical simulations or experiments.

We must, however, also recognize that V is a random number, being the matrix element of the coupling between modes of the two rooms. Thus, $\lim_{t\to\infty}\langle E_2\rangle/E$ is more properly written as $D\pi\langle|V|\rangle$. As $\langle V^2\rangle$ is related to the initial leaking rate σ, we can write this as

$$\lim_{t\to\infty}\langle E_2\rangle/E = (\pi\sigma D/2)^{1/2}[\langle|V|\rangle/\langle V^2\rangle^{1/2}], \qquad (28)$$

which describes the ultimate partition of energy as proportional to the square root of the dimensionless conductance σD, ie., in terms of the initial leaking rate times the modal density, and a numerical factor of order unity related to the statistics of V.

We will consider two forms that V's statistics might take. For each form we make detailed predictions for (1) the asymptotic energy level in room 2, and (2) the manner in which E_2 approaches its asymptote.

If the coupling is confined to a single point then V ought to be the product of the two modal amplitudes at that point and therefore V should be the product of two independent centered Gaussian random numbers. We write these two random numbers as x and y, each with identical p.d.f.

$$p(x)\,\mathrm{d}x = \exp\{-x^2/2\langle V^2\rangle^{1/2}\}/\sqrt{2\pi}\langle V^2\rangle^{1/4}\,\mathrm{d}x \tag{29}$$

such that $V = xy$, and $\langle V^2\rangle = \langle x^2\rangle\langle y^2\rangle$. The average of $|V|$ is obtained directly:

$$\langle |V|\rangle = \langle |xy|\rangle = (2/\pi)\langle V^2\rangle^{1/2}, \tag{30}$$

allowing the conclusion

$$\lim_{t\to\infty} \langle E_2\rangle/E = (\pi\sigma D/2)^{1/2}[\langle |V|\rangle/\langle V^2\rangle^{1/2}] = (2\sigma D/\pi)^{1/2}. \tag{31}$$

At intermediate times the average of equation (26) over all values of V is more demanding. On taking a time derivative of equation (26) one finds

$$\frac{\mathrm{d}\langle E_2\rangle}{\mathrm{d}t} = 2EDV^2\int_{-\infty}^{\infty}\mathrm{d}\beta\,\frac{\sin(2\sqrt{1+\beta^2}tV)}{\sqrt{1+\beta^2}} = 2\pi EDV^2 J_0(2t|V|), \tag{32}$$

On averaging over V this becomes

$$\frac{\mathrm{d}\langle E_2\rangle}{\mathrm{d}t} = \frac{ED}{\langle V^2\rangle^{1/2}}\int_{-\infty}^{\infty}\int_{-\infty}^{\infty} x^2y^2 \mathrm{J}_0(2t|xy|)\exp\{(-x^2-y^2)/2\langle V^2\rangle^{1/2}\}\,\mathrm{d}x\,\mathrm{d}y$$

$$= 32ED\langle V^2\rangle\int_0^{\infty}\int_0^{\infty} x^2y^2\mathrm{J}_0(4t\langle V^2\rangle^{1/2}|xy|)\exp\{-x^2-y^2\}\,\mathrm{d}x\,\mathrm{d}y, \tag{33}$$

an expression which may be evaluated in terms of elliptic integrals [16]:

$$\frac{\mathrm{d}\langle E_2\rangle}{\mathrm{d}t} = \frac{32ED\langle V^2\rangle}{[4+\xi^2]^{3/2}}\int_0^{\pi/2}\frac{1-2\xi^2\sin^2\theta/[4+\xi^2]}{\sqrt{1-\xi^2\sin^2\theta/[4+\xi^2]}}\,\mathrm{d}\theta, \qquad \xi \equiv 4t\langle V^2\rangle^{1/2}. \tag{34}$$

This integral is done numerically. It is plotted in Figure 2, versus non-dimensional time $\xi = 4t\langle V^2\rangle^{1/2}$, in units of $32ED\langle V^2\rangle$. Its antiderivative, being E_2 itself, is also plotted, in units of $8DE\langle V^2\rangle^{1/2}$. It is seen that the energy in room 2 overshoots its asymptotic level by 5·5%, achieving its maximum at a time $t \sim 1{\cdot}09/\langle V^2\rangle^{1/2} = (1{\cdot}09/\sigma)(2\pi D\sigma)^{1/2}$. There is a time scale for the approach to the maximum, that may be quantified by $t_{characteristic} = 0{\cdot}2677/\langle V^2\rangle^{1/2}$, being the time at which E_2 achieves 67% of its maximum value. The overshoot can be thought of as a remnant of a beat pattern, substantially smoothed by averaging over values of V. The overshoot is a prediction that could perhaps be confirmed in experiments. The 5·5% effect is

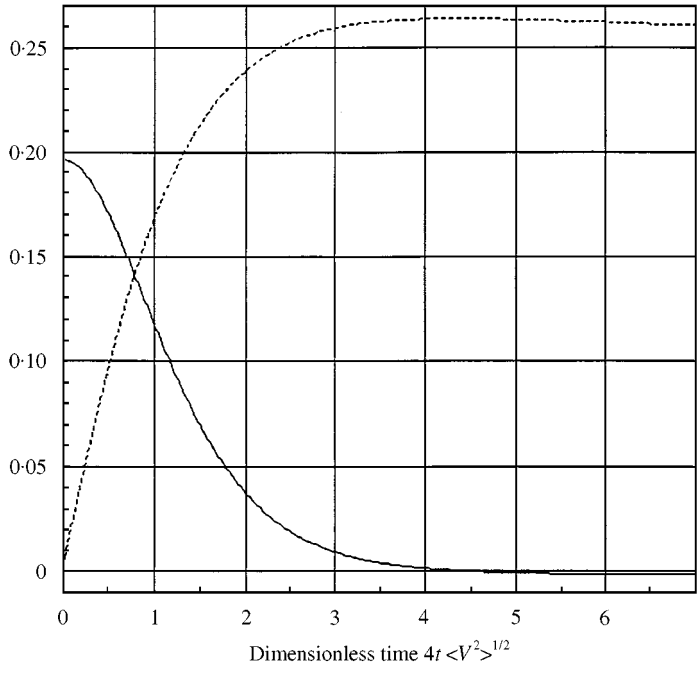

Figure 2. Evolution of the energy in room 2 for the case that V has the statistics of the product of two Gaussian random numbers. The dashed curve shows E_2 in units of $8DE\langle V^2\rangle^{1/2}$; it asymptotes to a value of $\frac{1}{4}$. The solid curve shows its time derivative, in units of $32ED\langle V^2\rangle$.

slight though, and the maximum is followed by a very slow relaxation towards the value at $t = \infty$ (reaching a point within 1% of the asymptotic value at $t = 5{\cdot}25/\langle V^2\rangle^{1/2}$.) The overshoot may be difficult to detect.

If there is reason to think that V is the sum of a large number of independent random numbers, then the central limit theorem indicates that V's statistics ought to be Gaussian. One therefore writes

$$p(V)\,\mathrm{d}V = \exp(-V^2/2\langle V^2\rangle)\,\mathrm{d}V/(2\pi\langle V^2\rangle)^{1/2} \tag{35}$$

and finds

$$\langle |V| \rangle = (2/\pi)^{1/2}\langle V^2\rangle^{1/2}. \tag{36}$$

Therefore,

$$\lim_{t\to\infty} \langle E_2\rangle/E = (\pi\sigma D/2)^{1/2}[\langle |V| \rangle/\langle V^2\rangle^{1/2}] = (\sigma D)^{1/2}, \tag{37}$$

which may be compared to equation (31). We see that different assumptions about the statistics of V lead to slightly different predicted proportionalities between $\sqrt{D\sigma}$ and the ultimate amount of energy in room 2.

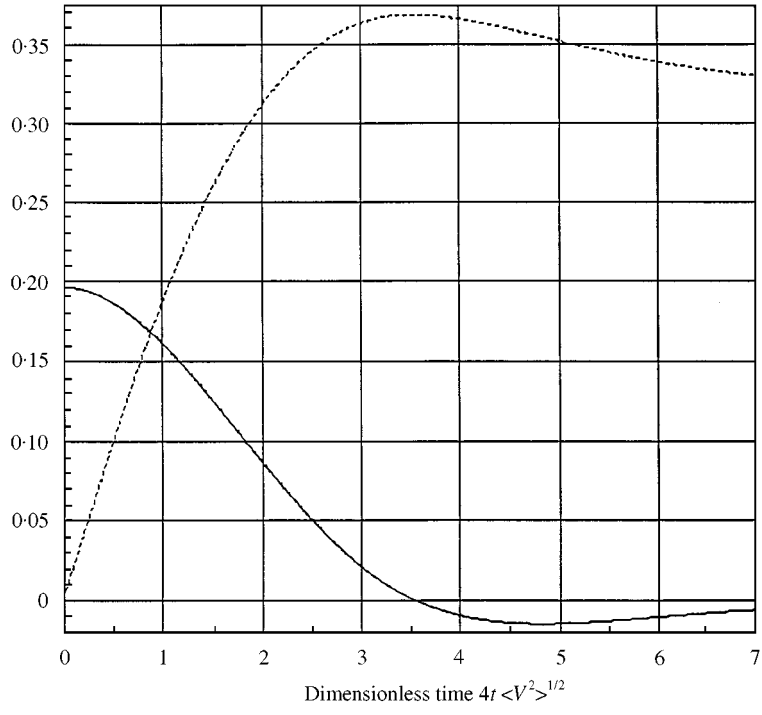

Figure 3. Evolution of the energy in room 2 in the case that V is itself a Gaussian random number. The dashed line shows E_2 in units of $8DE\langle V^2\rangle^{1/2}$; it asymptotes at a value of $\sqrt{2\pi}/8 = 0{\cdot}31333$. The solid line shows its time derivative, in units of $32ED\langle V^2\rangle$.

At intermediate times we average equation (32) to obtain [16, eqn. 2.12.9(1)]

$$\frac{\mathrm{d}\langle E_2\rangle}{\mathrm{d}t} = \int_{-\infty}^{\infty} 2\pi EDV^2 \mathrm{J}_0(2t|V|)\frac{\exp\{-V^2/2\langle V^2\rangle\}}{(2\pi\langle V^2\rangle)^{1/2}}\,\mathrm{d}V$$

$$= 2\pi ED\langle V^2\rangle \exp\{-\langle V^2\rangle t^2\}$$

$$\times[(1-2\langle V^2\rangle t^2)\mathrm{I}_0(\langle V^2\rangle t^2) + 2\langle V^2\rangle t^2 \mathrm{I}_1(\langle V^2\rangle t^2)], \qquad (38)$$

where I_n is the modified Bessel function of the first kind.

This expression is evaluated and plotted in Figure 3 versus non-dimensional time $\xi = 4\langle V^2\rangle^{1/2}t$, in units of $32ED\langle V^2\rangle$. Its antiderivative, being E_2 itself, is plotted also, in units of $8DE\langle V^2\rangle^{1/2}$. Again it is seen that E_2 overshoots its ultimate value (0·313 in the plot), in this case achieving its maximum at a time $\xi = 3{\cdot}555$ or $t = 0{\cdot}889\langle V^2\rangle^{-1/2}$. In this case it overshoots by 17·5%, an amount that may be less difficult to detect than the 5·5% overshoot predicted by the other model. The value to which E_2 ultimately relaxes is achieved much later; not until $t = 3{\cdot}38/\langle V^2\rangle^{1/2}$ is E_2 within 1% of its final value.

The two models for the statistics of V make predictions which differ in quantitative details, but they concur in predicting that the energy is not

equipartitioned, even at asymptotically late times, and they concur in predicting a degree of overshoot as the energy in room 2 approaches its steady state value. Neither of these features can be obtained from an SEA-like diffusion model.

4. NUMERICAL SIMULATION

To confirm these predictions we have studied the transient vibrations of a pair of coupled large two-dimensional meshes (Figure 1(a)). The system may be thought of as a spatially central-differenced version of a pair of coupled membranes, or as a spatially exact treatment of a pair of coupled meshes consisting of inertialess strings and point masses. We have studied such systems before [17]. In each "room" the dynamics of site (i, j) are governed by the differential equation

$$\frac{\mathrm{d}^2}{\mathrm{d}t^2} u_{ij} + (4u_{ij} - u_{ij-1} - u_{i-1j} - u_{ij+1} - u_{i+1j}) = 0. \tag{39}$$

The site indexes i, j have ranges that depend on the chosen size of the room, typically 200×200. The displacement is set to zero on the boundary of the room, a boundary that is randomly rough, in the fashion described in reference [17]. Each room was given a different rough boundary. It is this difference between the rooms that constitutes the disorder needed for localization. (In the absence of a difference between the rooms, the modes of each room separately would be identical, $\alpha = \omega$; the coupling would couple degenerate modes; all modes of the composite would be equipartitioned and thus the diffuse fields would be also.) At extremely low frequencies, with wavelengths long compared to the scale of the rough boundary, the rooms appear identical and we would therefore expect equipartition to be recovered.

The above equation was solved by central differences in time, from an initial condition consisting of a unit velocity on the chosen source site in room number 1. A time step size of 0·47 was chosen, about 50% more conservative than the value need to ensure stability. This choice of time step also served to minimize, for the frequencies of interest, dispersion from the time stepping.

The rooms were coupled in a variety of fashions. In one version the rooms were coupled by setting, at each time step, the displacements in each room equal along a chosen "stitch". In another version the rooms were coupled by supplementing equation (39) with an additional force on the sites along the stitch, a force proportional to the difference in displacements of the sites in the stitch between the rooms, thus modelling the coupling between the rooms by means of a short row of springs connecting the rooms. Stitch lengths were typically 4–6. The results from these two versions are similar to those of the third and fourth versions, for which we present detailed results.

In a third version (Figure 1(a)) the rooms are coupled by means of a window, of length 6 sites, set in the wall of each room. This case corresponds most closely to the usual picture of coupled reverberation rooms, and to the system studied in our experiments. In a fourth version (not shown), we couple the rooms by connecting

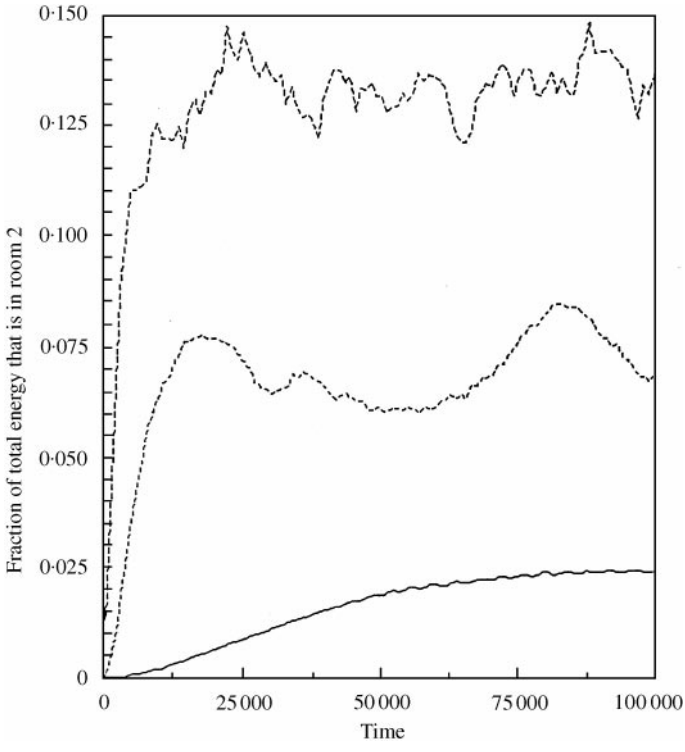

Figure 4. For the case in which the rooms are coupled by a small window, the fraction of the energy that is in room 2 is plotted versus time for the three lowest bins. ——, Bin 1; - - - -, bin2; – – –, bin 3.

each of a set of several randomly chosen site pairs of the two rooms by a weak spring.

In each version, the displacement $u(t)$ was recorded for each of 16 chosen receiver sites in each of the two rooms. Each such record was cosine-bell time-windowed, Fourier-transformed, and integrated over 16 distinct short ranges in frequency. The result, for each receiver, was an array of spectral power density versus time and frequency. The power densities from each of the 16 receivers in each room were then added to give an estimate for each room's average spectral power density, as a function of time and frequency. Thus, quantities proportional to $E_1(t)$ and $E_2(t)$ for each of 16 frequency bins were constructed. The values so constructed inevitably have fluctuations, as the receivers sample only the signal at their positions, but simple arguments suggest that the (spatial and frequency) averaging we do, combined with averaging over 15 configurations, should have been sufficient to reduce these fluctuations to about 2%.

4.1. ROOMS COUPLED BY A WINDOW

In Figures 4–7 we plot the results of the numerical simulation of two coupled reverberation rooms, coupled by a window. These figures show the evolution of the

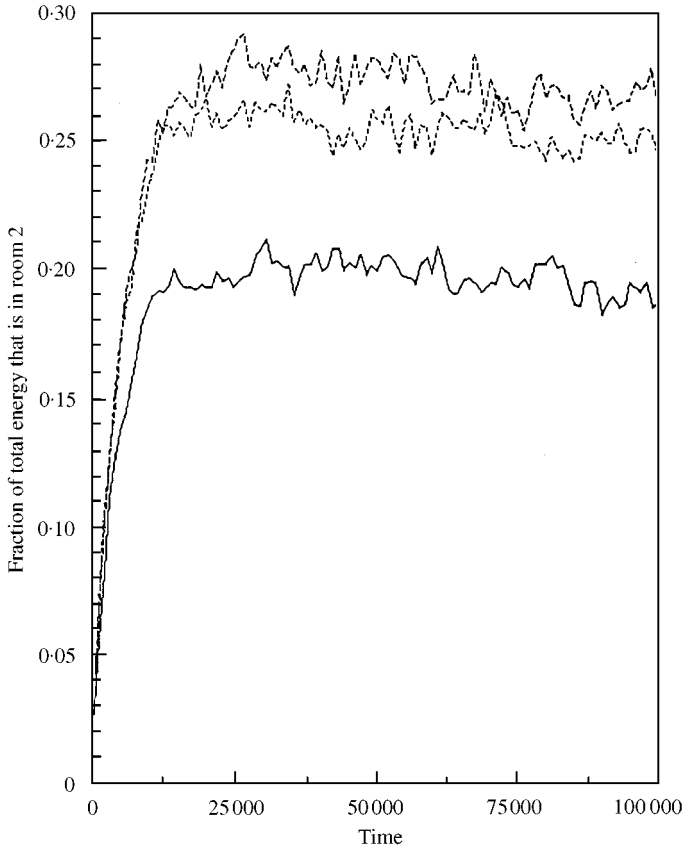

Figure 5. For the case in which the rooms are coupled by a small window, the fraction of the energy that is in room 2 is plotted versus time for bins 4 (bottom curve), 5 (middle curve) and 6 (top curve).

energy in a pair of 207×207 rooms, each with boundary roughness with a maximum depth of 9. The quantity E_2/E is plotted, versus time, for each of 16 frequency bins. These bins span a range of wavelengths from 40 (at the midpoint of bin 2) to 4·0 (at the midpoint of bin 16), thus spanning a wide range in comparison to window size. Except in bins 1 and 2, the wavelengths are much smaller than room size.

In each bin, except for bins 1 and 2 for which the room is perhaps too small for statistical treatment, the predictions of the theory are corroborated. We see a degree of localization that varies from strong at low frequencies (where modal density D is small) to weak at high frequencies (where D is great.) In bin 5 for example, the late time value of E_2/E appears to be about 0·25, less than the equipartition value of 0·50. We see a smooth transition as E_2 rises from zero to its asymptote. The predicted overshoot is apparent also, in bins 4–10. At low frequencies, in bins 1–3, the overshoot is not obvious, but the other peculiarities of these low frequencies, presumably related to the small ratio of room size to wavelength, would mask the small overshoot effect. At high frequencies the overshoot is rather weak. It may be that the violation of the strong localization

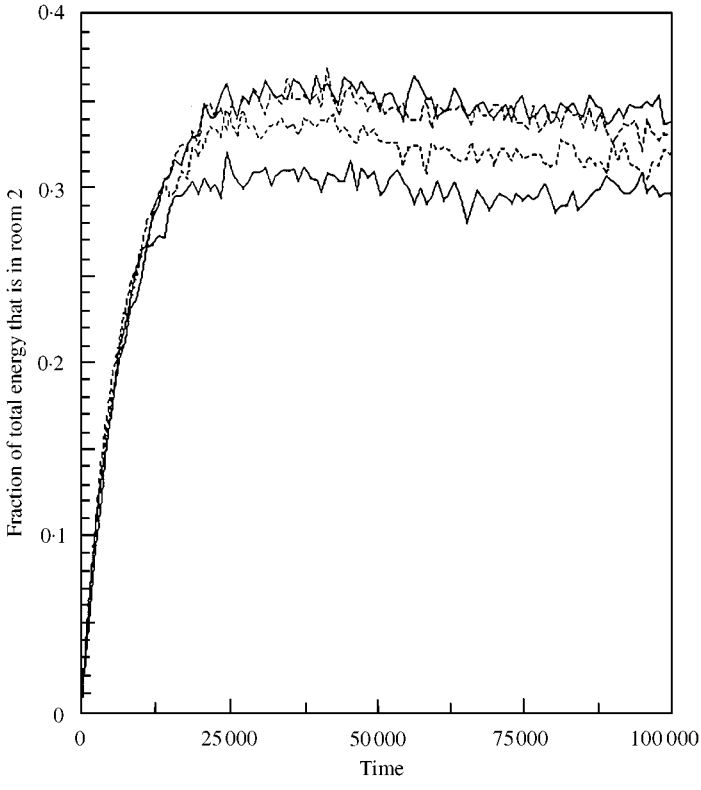

Figure 6. For the case in which the rooms are coupled by a small window, the fraction of energy in room 2 associated with bins 7 (bottom curve), 8, 9, and 10 (top curve).

assumption, made just prior to equation (21) is responsible. It may be that the overshoot is difficult to detect because the relaxation to the ultimate value is so slow.

We also investigate prediction (31). Modal densities D are estimatable from an approximation that our structure has no dispersion or anisotropy (approximately true at these frequencies) using the standard formula for modal density in a square Dirichlet membrane,

$$D = \Omega A/2\pi c^2 - L/4c. \tag{40}$$

Setting $A = (207 - 9)^2$, $c = 1$, $L = 207–9$, taking σ from the early time slopes of the curves shown in Figures 4–7, and taking the late time value of E_2/E_{total} from the average value of the curves shown in these figure between times 90 000 and 100 000, we construct Table 1.

The agreement with theory continues to be remarkable. The degree of localization is well approximated by the estimate $(2\sigma D/\pi)^{1/2}$. That the estimate is consistently higher than the observations, i.e., that localization is more severe than predicted by about 20% is not a serious flaw; the theory took the coupling to be of the simple form of a small perturbation in the stiffness matrix. The simulated system

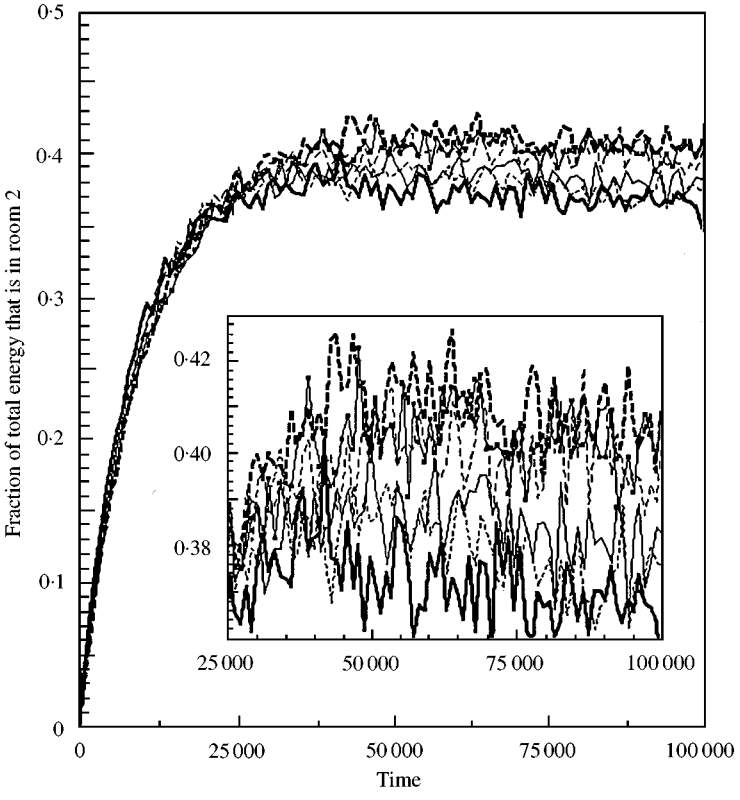

Figure 7. For the case in which the rooms are coupled by a small window, the fraction of the energy that is in room 2 is plotted versus time for bins 11–16: ——, bin 11; - - - -, bin 12; ——, bin 13; – – –, bin 14; ■–■–■, bin 15; ▬ ▬ ▬, bin 16.

consisting of a transparent window between the two rooms is not, however, readily put in that form.

4.2. ROOMS COUPLED BY SEVERAL SPRINGS

Numerical simulations were also carried out for a system consisting of a similar pair of reverberation rooms, but coupled by a set of $n_{spring} = 12$ springs, each of stiffness $K = 0{\cdot}16$, placed at random positions. This system is one for which V should be a Gaussian random number, with a mean-square value that can be estimated *a priori*.

In such a system the matrix element of $\boldsymbol{v}$ between site (i, j) of room 1 and site (l, k) of room 2 is zero unless $(i, j) = (l, k)$, and unless (i, j) is one of the n_{spring} sites on which a spring of stiffness K has been placed. It is equal to $-K/2\Omega$ otherwise. Thus the quantity V is given by

$$V_{nv} = \boldsymbol{\psi}^n \cdot \boldsymbol{v}\boldsymbol{\phi}^v = -(K/2\Omega) \sum_{s=1}^{n_{spring}} \psi^n_{i_s j_s} \phi^v_{i_s j_s}. \tag{41}$$

TABLE 1

Parameters of the waves and the transport taken from the numerial simulation of the rooms coupled by a window

Bin	Central ω	λ	σ	D	E_2/E_{total} at $t = 10^5$	$(2\sigma D/\pi)^{1/2}$
1	0·052065	121	2·59e-8	275		0·002
2	0·156195	40	2·33e-6	925	0·0715	0·37
3	0·260325	24	3·99e-5	1575	0·136	0·200
4	0·364455	17	4·49e-5	2225	0·189	0·252
5	0·468585	13·4	6·16e-5	2875	0·250	0·307
6	0·572715	11·0	4·66e-5	3525	0·268	0·323
7	0·676845	9·3	4·92e-5	4174	0·300	0·362
8	0·780975	8·0	4·87e-5	4824	0·315	0·387
9	0·885105	7·1	4·74e-5	5474	0·332	0·406
10	0·989235	6·35	4·59e-5	6123	0·345	0·423
11	1·09336	5·7	4·40e-5	6773	0·366	0·436
12	1·19749	5·25	4·46e-5	7423	0·375	0·459
13	1·30163	4·8	4·36e-5	8073	0·380	0·473
14	1·40576	4·5	4·10e-5	8722	0·395	0·477
15	1·50988	4·2	3·89e-5	9372	0·400	0·482
16	1·61401	3·9	3·66e-5	10022	0·405	0·483

This is the sum of n_{spring} random numbers, each of which is the product of two centered Gaussian random numbers, each with the mean square given by the normalization of the pseudo-modes. $\langle \psi^2 \rangle = \langle \phi^2 \rangle = 1/N$, where N is the number of sites in each room. If n_{spring} is sufficiently large, then the central limit theorem tells us that V should be a centered Gaussian random number, with a mean square equal to the sum of the mean squares of the terms composing V. Thus,

$$\langle V^2 \rangle = (K/2\Omega)^2 \frac{n_{spring}}{N^2}. \tag{42}$$

The theory above then predicts that the initial leaking rate σ is $2\pi D \langle V^2 \rangle$. The modal density is given by equation (40), so we estimate

$$\sigma = \frac{n_{spring}}{N} \frac{K^2}{4\Omega} = 2 \times 10^{-6}/\Omega, \tag{43}$$

a leaking rate that scales inversely with frequency.

We furthermore predict that the localization fraction, in accord with equation (37), should be $(\sigma D)^{1/2}$, or

$$E_2/E \to \sqrt{\frac{K^2 n_{spring}}{4}} = 0{\cdot}156, \tag{44}$$

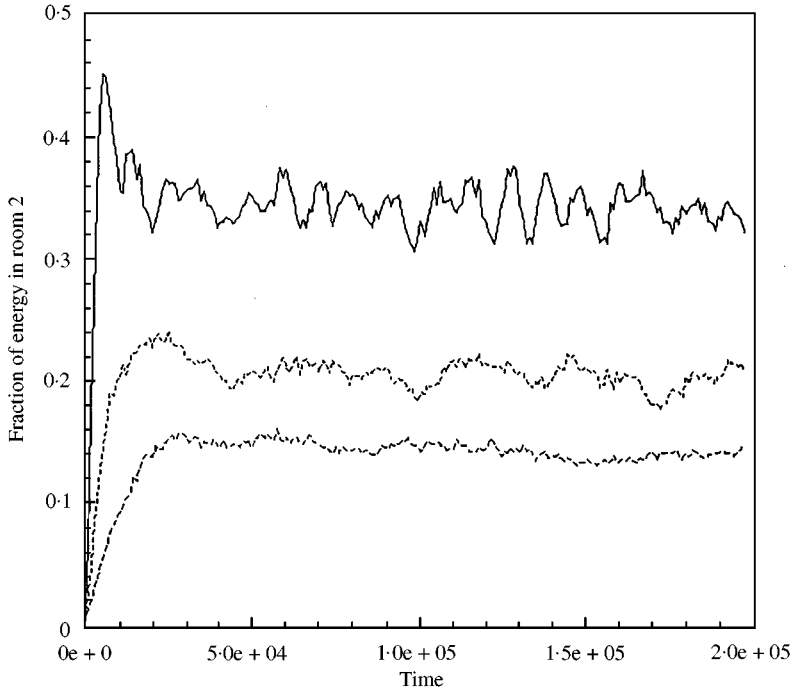

Figure 8. The fraction, of the total energy, that resides in room 2. Results in bins 2 (top curve), 3 and 4 (bottom curve) from a numerical simulation of a pair of 207×207 rooms with roughness 9; 12 spings of stiffness 0·16 each couple the rooms.

independent of frequency. The energy in room 2 is expected to overshoot its asymptotic value by about 17%.

The results of the numerical simulations are shown in Figures 8–10. The initial slopes have been estimated from the numerical results, and may be compared with prediction (20). In bins 4 and below, the initial slope is difficult to measure, but for bins 5–10 it is readily found. They are, respectively, 5×10^{-6}, 3·6, 3·0, 2·7, 2·45 and 2·2; each with an uncertainty of about 0·1. Equation (20) on the other hand, predicts 4·3, 3·51, 2·94, 2·56, 2·25 and 2·02. These are not in perfect agreement, but are close enough that we may attribute the differences to Monte Carlo fluctuations or to minor errors in the model. The observed initial leaking rates appear to be consistently greater than predicted, albeit by only $\sim$10%.

The asymptotic values of the partition of energy may also be compared with equation (44). In the numerical simulations, bins 2, 3 and 4 have asymptotic values of about 0·35, 0·20 and 0·14 respectively. Bins 5–10 all have asymptotic values of about 0·11. At higher frequencies it is not obvious that the asymptote has been achieved, its value therefore cannot be estimated. In any case it is clear that the numerical simulations do show localization, but the degree of localization is mispredicted by our theory, by about 30%.

Overshoot is observed, but not in precise accord with theory. The lower frequencies, bins 2–7, show overshoots of 32, 20, 11, 14, 12 and 8% respectively. For the higher bins overshoot is difficult to estimate; but it appears to be significantly less than the predicted 17%.

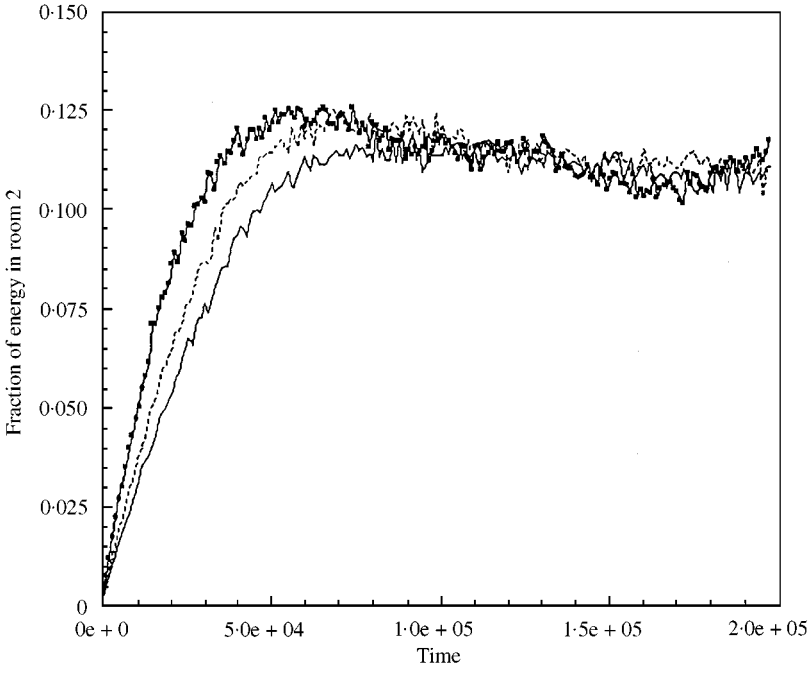

Figure 9. The results in bins 5 (top curve), 6, and 7 (bottom curve) from the system of Figure 8.

There are minor discrepancies between theory and the results of the numerical simulations. It is outside the scope of this communication to pursue the causes of these minor quantitative discrepancies. Nevertheless, one may speculate that, as theory assumed that localization was strong, non-infinitesimal values of $\sqrt{\sigma D}$ may be responsible for the disagreements. Alternatively, it may be that the statistics of V are not Gaussian, that the central limit theorem does not apply, either because there are correlations between the sites on which the springs have been placed (due to finite wavelength and finite system size) or because $n_{spring} = 12$ is not a sufficient number of coupling springs.

5. EXPERIMENTS

In order to demonstrate the effect in the laboratory a small aluminum block, as pictured in Figure 1(b), was constructed. It had nominal dimensions of $25{\cdot}4 \times 25{\cdot}4 \times 50{\cdot}8$ mm, but was nearly severed by some mm wide cuts in the midplane that left the two halves joined by a residual ligament of dimensions $2{\cdot}2 \times 2{\cdot}2 \times 1$ mm. Other short oblique cuts and spherical surfaces, as pictured, were added in order to break the reflection and rotation symmetries and enhance the generation of a diffuse field.

The structure was insonified and monitored with piezoelectric point transducers (dry-coupled Valpey–Fisher pin transducers) with useful bandwidth from 0·1 to

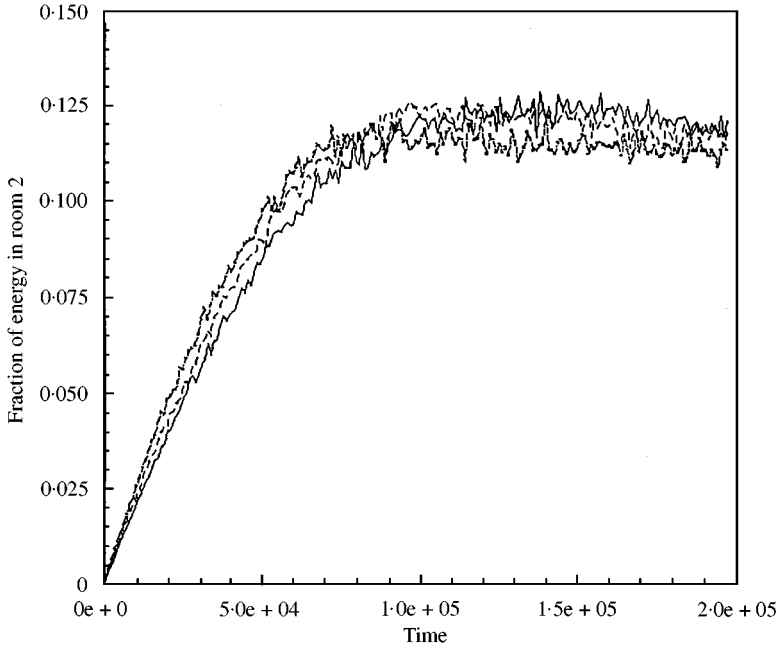

Figure 10. The results from bins 8–10, for the system of Figure 8.

2·0 MHz. If the transducers were ideal and well calibrated, it would be sufficient to use one transducer, e.g. the one labelled A in the figure, as an impulsive source, and use transducers B and 1 to receive. Localization would manifest as a greater spectral energy density in receiver B than in receiver 1. If, however, B and 1 had different sensitivities, the effect we seek would be compromised. In order to mitigate the effect of variable transducer sensititivity we opted for the pictured 4-transducer scheme. We constructed the energy ratio

$$\sqrt{\frac{(A1)(B2)}{(AB)(12)}}, \tag{45}$$

where the notation (XY) signifies the spectral energy density in receiver Y due to the impulsive source acting in transducer X. The quantity may be interpreted as the ratio of energy in room 2 to that of room 1. It should have a zero value at zero time, but increase to a late time value of unity in the non-localized regime. In the localized case it should approach an asymptote that is less than unity. At the expense of introducing additional stochastic fluctuations, the construction of this ratio serves to remove the effect of transducer sensitivity. Assuming that each half of the structure has the same absorptivity, the ratio also eliminates the effect of absorption.

A ray picture serves to allow an estimate of the initial leaking rate that is, barring diffraction corrections, independent of frequency. Applying equation (3) with the shear wave speed (as the majority of the energy is in the form of shear waves) we

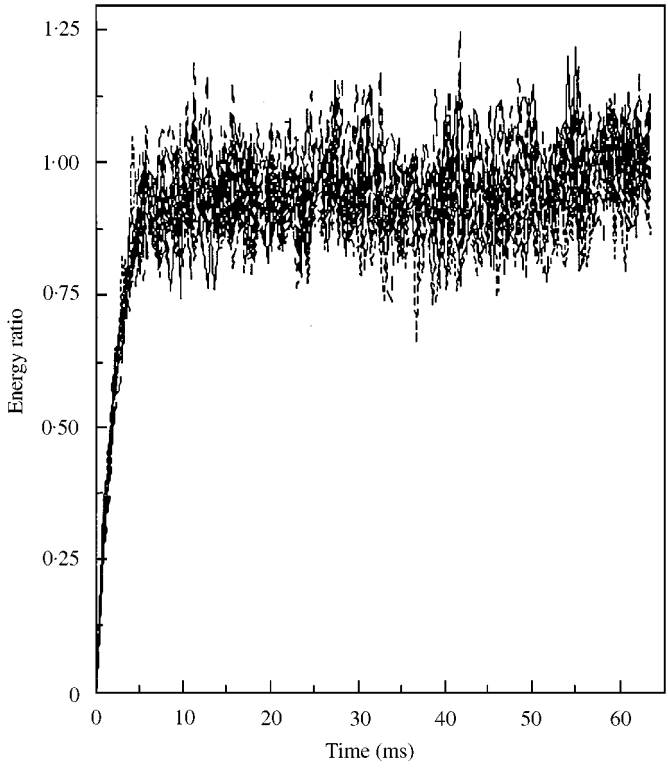

Figure 11. The energy ratio, between the energy in room 2 and 1, observed in the ultrasonic experiments at the higher frequencies, between 898 and 1835 kHz. At these short wavelengths the system is predicted not to localize and that is indeed what is observed. All 13 bins plotted here have essentially identical behavior.

find that the initial leaking rate is estimated to be 0·24/ms. Diffraction corrections could modify this estimate if wavelengths are comparable to or greater than twice the window size of 2 mm, i.e., for frequencies below 750 kHz. As discussed above, the significance of diffraction corrections is also the sign of the significance of localization; thus we predict localization at frequencies substantially less than 750 kHz, and extended modes at frequencies substantially greater than 750 kHz. These predictions may be compared to observations.

The results, after spatial averaging, are plotted in Figures 11 and 12. In Figure 11 the energy ratio (45) is plotted versus time for the higher frequency bins. It is observed that all these higher bins have essentially the same behavior; identical initial leaking rates (of about 0·3/ms—slightly greater than the simple ray picture predicted) and identical asymptotic value of about unity. In Figure 12 the energy ratio (45) is plotted for the lower frequency bins, in the regime for which we expect localization. This is indeed observed; at 200 kHz, for example, the asymptotic energy in room two is only one-quarter that of room 1.

We may make a comparison of the observed late time asymptote, for example at 273 kHz where it takes a value of 0·5, with the theoretical expectation of order $\sqrt{\sigma D}$

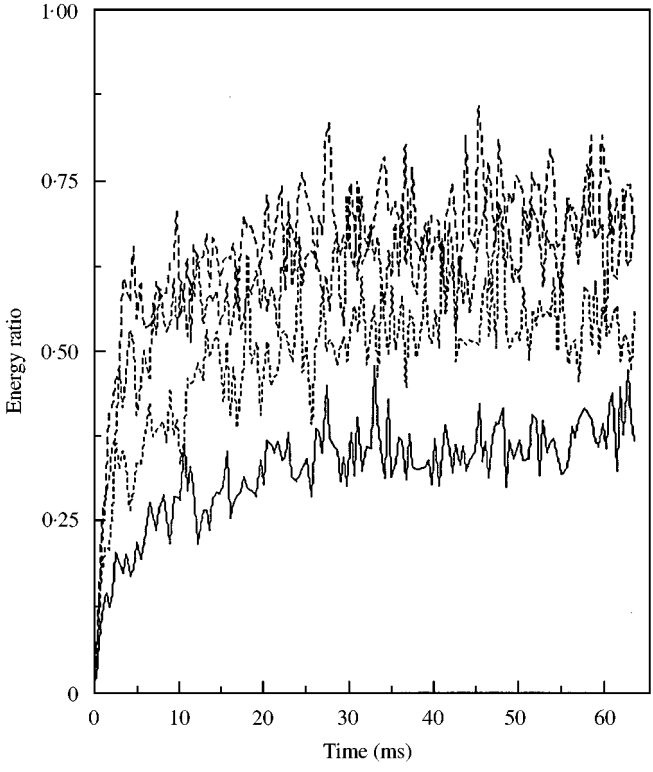

Figure 12. The energy ratio, between the energy in rooms 2 and 1, observed in the ultrasonic experiments at frequencies of 195 (lowest curve), 272, 351 and 429 (highest curve) kHz. At these wavelengths the system is predicted to localize and that is indeed what is observed. The asymptotic energy density in room 2 is significantly less than that of room 1, especially at the lowest frequencies.

based on equation (37). Taking D to have its usual Weyl value for elastic waves [18],

$$\mathrm{d}N/\mathrm{d}\omega = D(\omega) = (V/2\pi^2)\{\omega^2/c_d^3 + 2\omega^2/c_e^3]$$

$$+ (S\omega/8\pi c_d^2)[2-3(c_d/c_e)^2 + 3(c_d/c_e)^4]/[(c_d/c_e)^2 - 1] + O(L/c), \quad (46)$$

where the volume of each room V is $\sim (25{\cdot}4\,\mathrm{mm})^3$ and surface area S is $\sim 6\times(25{\cdot}4)^2$, we find that D, at 273 kHz is 0·26 ms. The leaking rate may be estimated from equation (3) by neglecting diffraction effects, or taken from the slope of the energy ratio at the earliest time; in both cases one obtains about 0·24. Thus $\sqrt{\sigma D}$ is about 0·25, significantly less than the observed asymptotic energy ratio of 0·5. This bin shows, furthermore, a peculiar and unpredicted slow approach to its asymptote. It is as if the proper asymptote $\sim 0{\cdot}25$ is achieved at early times ($\sim$10 ms, as in Figures 2 and 3, at a time of order $3/\sigma$) and then a different mechanism acts to augment the ratio over much longer times (and incidentally to thereby mask the predicted overshoot as well). The anomalous behavior is reminiscent of that observed in an earlier ultrasonic study [12] of Anderson

localization in a disordered two-dimensional system. Here we content ourselves with recognition of the substantial concurrence between theory and measurement, and relegate resolution of the minor discrepancies to later work.

6. CONCLUSIONS

It has been shown theoretically, and demonstrated in numerical simulations and in laboratory ultrasonic experiments, that energy flow in weakly coupled reverberant systems can be Anderson localized. The effect is significant when the energy flow rate (in units of inverse time) is comparable to or less than modal spacings. In the case that the rooms are coupled by a transparent window, the criterion is equivalent to wavelength being comparable to or greater than window size.

ACKNOWLEDGMENTS

This work was supported by grant number 9701142 from the National Science Foundation.

REFERENCES

1. R. H. Lyon and R. G. DeJong 1995 *Theory and Application of Statistical Energy Analysis*, Boston, MA: Butterworths-Heimann.
2. M. L. Lai and A. Soom 1990 *Journal of Vibration and Acoustics* **112**, 127–137. Prediction of transient vibration envelopes using SEA techniques.
3. R. J. Pinnington and D. Lednik 1996 *Journal of Sound and Vibration* **189**, 249–264. Transient SEA of an impulsively excited two oscillator system.
4. C. H. Hodges 1982 *Journal of Sound and Vibration* **82**, 411. Confinement of vibration by structural irregularity.
5. C. H. Hodges and J. Woodhouse 1986 *Reports on Progress in Physics* **49**, 107–170. Theories of noise and vibration transmission in complex structures.
6. C. Pierre 1990 *Journal of Sound and Vibration* **139**, 11. Weak and strong localization in disordered structures: a statistical investigation.
7. D. Li and H. Benaroya 1992 *Applied Mechanics Review* **45**, 447–459. Dynamics of periodic and near-periodic structures.
8. W.-C. Xie and X. Wang 1997 *AIAA Journal* **35**, 1645–1652. Vibration mode localization in one-dimensional systems
9. R. Weaver 1996 *Localization and the Effects of Irregularities in Structures*, *Applied Mechanics Reviews* **49**, 111–120. Localization, scaling, and diffuse transport of wave energy in disordered media.
10. R. L. Weaver and J. Burkhardt 2000 *Solitons Chaos and Fractals.* Transport in multi-coupled Anderson localizing systems (in press).
11. W. Kohler and G. Papanicolaou 1973 *Journal of Mathematical Physics* **14**, 1733–1745, Power statistics for wave propagation in one dimension and comparison with radiative transfer theory.
12. R. Weaver 1990 *Wave Motion* **12**, 129–142. Anderson localization of ultrasound.
13. R. L. Weaver 1994 *Physical Review B* **49**, 5881–5895. Anderson localization in the time domain: numerical studies of waves in two-dimensional disordered media.
14. E. Abrahams, P. W. Anderson, D. C. Licciardello and T. V. Ramakrishnan 1979 *Physical Review Letters* **42**, 773–676. Scaling theory of localization: absence of quantum diffusion in two dimensions.

15. P. W. Anderson 1958 *Physical Review* **109**, 1492–1505. The absence of diffusion in certain random lattices.
16. A. P. Pridnikov, Y. A. Brychkov and O. I. Marichev 1983 *Integrals and Series. Special Functions*, eqn 3.2.4(27). Moscow Science.
17. R. Weaver and J. Burkhardt 1994 *Journal of the Acoustical Society of America* **96**, 3186–3190. Weak Anderson localization and enhanced backscatter in reverberation rooms and quantum dots.
18. R. Weaver 1989 *Journal of the Acoustical Society of America* **85**, 1005–1013. Spectral statistics in elastodynamics.